International Journal of Pharmaceutics 683 (2025) 126062

Contents lists available at ScienceDirect

International Journal of Pharmaceutics

journal homepage: www.elsevier.com/locate/ijpharm

Electrospun membranes from natural polymers with Quercetin: design and characterization, antioxidant and antimicrobial activity, and potential for skin reinnervation in chronic wounds

Catarina Correia [a], Ana Sofia Pádua [a], Catarina Matela [b], Inês C. Gonçalves [d,e], Paula Soares [a,c], Célia Henriques [a,b], Isabel Sá-Nogueira [d,e], Jorge Carvalho Silva [a,b], Tânia Vieira [a,b,*]

[a] Centro de Investigação de Materiais, Institute for Nanostructures, Nanomodelling and Nanofabrication, CENIMAT/i3N, Portugal
[b] Physics Department, School of Science and Technology, Nova University of Lisbon, Lisbon, Caparica 2829-516, Portugal
[c] Material Science Department, School of Science and Technology, Nova University of Lisbon, Lisbon, Caparica 2829-516, Portugal
[d] Applied Molecular Biosciences Unit, UCIBIO, Associate Laboratory i4HB, Portugal
[e] Department of Life Sciences, School of Science and Technology, Nova University of Lisbon, Lisbon, Caparica 2829-516, Portugal

ARTICLE INFO

Keywords:
Antimicrobial
Antioxidant
Electrospinning
Neuronal differentiation
Quercetin
Wound healing

ABSTRACT

The rising problem of chronic wounds demands the investigation of therapeutic solutions that are easy to use, target microbial infection and excessive reactive oxygen species (ROS) at the wound site, and account for skin reinnervation. The aim of this research was to develop electrospun membranes from natural polymers – chitosan (CS) and fish gelatin (FG) – crosslinked with citric acid, incorporating quercetin as an active pharmaceutical ingredient (API) to enhance its therapeutic potential. The produced membranes exhibited a uniform morphology and a cross-shaped network, providing porosity and the ability to sustain hydrolytic degradation. Drug delivery assays revealed a higher release percentage at pH 7.4 and pH 8, which correspond to wound site conditions. However, quercetin degradation at this pH suggests the need for encapsulation. Antioxidant activity analysis confirmed quercetin's great antioxidant capabilities, reaching up to 93.71 ± 0.92 % for pure quercetin, and 53.77 ± 3.09 % for quercetin-containing fibers. Neuronal differentiation assays demonstrated quercetin's ability to promote neuronal differentiation. Antibacterial activity was tested for the membranes against *Escherichia coli* (*E. coli*) and Methycillin-resistant *staphylococcus aureus* (MRSA). The results showed a beneficial effect from incorporating quercetin into the membranes in reducing MRSA growth but no noticeable effects on *E. coli*. These findings highlight the potential of quercetin-loaded fibers for wound healing applications, with antioxidant, antibacterial, and neurogenic properties.

1. Introduction

Chronic skin wounds are a rising global problem, being responsible for a multitude of health complications, namely lower extremity amputations in cases of diabetic foot ulcers, with a high 5-year mortality rate, especially when combined with additional diseases (Armstrong et al., 2007). Chronic wounds occur when the wound healing process is carried out improperly, taking a long time to restore anatomic and functional integrity or even not advancing beyond the inflammatory phase, often resulting in persistent infection and impaired physiological healing mechanisms (Yao et al., 2020; Abrigo et al., 2014). Most of the treatments employed nowadays do not hold the capacity to regenerate and reinnervate chronic skin wounds, reestablishing the patient's quality of life. Instead, they mostly aid in wound repair and closure, which leads to skin with less strength and lack of functionality, increasing the probability of recurrence (Yao et al., 2020). Cutaneous reinnervation is essential for wound healing since the poor nerve regeneration of the skin leads to loss of sensibility, itch, paresthesia, pain, and delays the overall rehabilitation (Girard, 2017). Therefore, tissue engineering has been highly sought after to obtain adequate treatments for these kinds of wounds.

Electrospinning comes down as a promising technique due to its

* Corresponding author.
E-mail address: ts.vieira@fct.unl.pt (T. Vieira).

https://doi.org/10.1016/j.ijpharm.2025.126062
Received 9 June 2025; Received in revised form 19 July 2025; Accepted 8 August 2025
Available online 11 August 2025

ability to create fibrous structures with diameters ranging from a few nanometers to several micrometers (Abrigo et al., 2014; Agarwal et al., 2008; Schiffman and Schauer, 2007; Bhardwaj and Kundu, 2010; Azimi, et al., 2020). These present high surface area and porosity, making them suitable candidates for tissue engineering applications since they can mimic the extracellular matrix and serve as a supportive network for cell adhesion and proliferation (Agarwal et al., 2008). These aspects also contribute to good oxygen permeability and gas exchange, which are important factors in wound healing (Karuppannan, 2022; Zhong et al., 2010). Choosing the optimal polymer, or combination of polymers, is essential to obtain a fiber capable of fulfilling the desired purpose. Chitosan (CS) is a polymer derived from chitin and one of the most abundant biopolymers, being the only positively charged (Ficai et al., 2016; Cui, et al., 2021). It has multiple properties that make it an interesting candidate for tissue engineering applications, namely being bioactive, biodegradable, and biocompatible, as well as having low antigenic and anti-bacterial properties (Oryan et al., 2016; Ficai et al., 2016). However, there are some drawbacks, such as its poor mechanical strength, which can be improved by combining CSwith other polymers, like gelatin, and providing crosslinking (Ficai et al., 2016). Gelatin is a natural polymer derived from collagen and is a blend of several water-soluble proteins. It contains many enticing properties, namely its good biocompatibility and biodegradability, as well as being non-antigenic, non-toxic, and adhesive (Oryan et al., 2016). Furthermore, the presence of unique aminoacid sequences promotes enhanced cell adhesion and proliferation (Mathew and Arumainathan, 2022). Its poor spinnability and mechanical properties can be overcome by combining with other polymers and performing crosslinking reactions.

Considering the characteristics of the wound bed, namely, its moisture and nutritious environment, which are favorable to bacterial growth, it is imperative that the developed treatment encompasses a strategy to minimize those effects. The previously described characteristics inherent to the nanofibers can help manage these conditions, as well as prevent the penetration of microbial agents (Karuppannan, 2022). However, incorporating a pharmaceutical component can be advantageous. Several studies have proven the antimicrobial efficacy of natural ingredients (Trinh et al., 2022), such as: propolis, which showed an increase in the anti-bacterial activity against *Escherichia coli* (*E. coli*) and *Staphylococcus aureus* (*S. aureus*) when incorporated in CS and gelatin nanofibers (Ribeiro et al., 2021); curcumin, which showed great efficacy in reducing the bacterial activity of *S. aureus* and extended spectrum β-lactamase producing bacteria when incorporated in polycaprolactone (PCL) and gum tragacanth fibers (Mohammadi et al., 2016). Quercetin is a polyphenolic flavonoid found in several foods and has been shown to exhibit numerous beneficial properties (Karuppannan, 2022; Da Silva Uebel, 2016). These include anti-oxidant and anti-inflammatory activity, as well as anti-bacterial activity (Karuppannan, 2022; Da Silva Uebel, 2016). Studies have also shown that quercetin can promote reinnervation by expressing specific factors and activating pathways involved in neuronal growth (Chen, 2017). Quercetin showed neuroprotective effects in rats with diabetic peripheral neuropathy, greatly improving their peripheral neurological functions through the expression of axonal growth factors (Song, 2024). Furthermore, *in vivo* studies showed the beneficial effects of quercetin on the microenvironment of the nervous tissue, by reducing inflammatory response and oxidative stress, which decrease neuropathic pain (Fideles et al., 2023). Nonetheless, this compound also has its drawbacks, mainly its low water solubility, degradation due to light exposure, and rapid metabolism when reaching systemic circulation (Karuppannan, 2022). Many have combined the activity of quercetin with other natural ingredients, like rutin (Stoyanova, 2022) and cyclodextrin (Kost, 2020). However, our study focuses solely on quercetin and demonstrating its properties when acting alone, which is advantageous not only regarding production costs but also in minimizing potential adverse effects. Furthermore, many studies incorporate quercetin in scaffolds produced with synthetic polymers, such as polylactide acid (PLA) or PCL (Darie-Niță et al., 2022), often performing crosslinking with chemical crosslinking agents, like glutaraldehyde (Hulupi and Haryadi, 2019). This is an additional aspect for which our produced scaffolds stand out, given they are produced solely by natural polymers, crosslinked with a natural agent (citric acid), and incorporate a natural active pharmaceutical ingredient (API).

Although other studies are found in literature including electrospun gelatin membranes crosslinked with citric acid (Liguori, 2019), electrospun membranes of PCL with PLA and polylactic-co-glycolic acid incorporating quercetin and films of CS (Eskitoros-Togay et al., 2018) and gelatin crosslinked with genipin that incorporate quercetin (Roy and Rhim, 2022), none of the studies use the combinations presented in this work in the form of electrospun membranes. This study combines polymers, a crosslinking agent, and an active ingredient which are all from natural origin avoiding the use of toxic and synthetic compounds. This fully natural-based approach demonstrated a reliable alternative and account for reinnervation, a missing part of the treatment of chronic wounds. Thus, this study highlights the potetial of quercetin to induce the neuronal differentiation, which is a must in their use for skin regeneration.

The current study aims to produce CS and fish gelatin (FG) electrospun fibers crosslinked with citric acid, incorporating quercetin as an API to enhance the healing potential of the proposed patches. To evaluate the efficacy of these patches, several tests were conducted to determine the physico-chemical characteristics of the fibers, as well as their biocompatibility. The API was also tested regarding its drug release kinetics, anti-oxidant and anti-bacterial activity, as well as the ability to promote neuronal differentiation.

2. Materials and methods

2.1. Membranes production

To produce the FG and CS (FGCS) polymeric fibers, the following polymer concentrations were used: FG (Sigma-Aldrich) and CS (Cognis, M_w = 500 kDa and a degree of deacetylation = 75.5 %) at a concentration of 2 % (w/w) each, and 0.2 % (w/w) of Polyethylene oxide (PEO, Sigma-Aldrich, M_v = 2,000,000). PEO was used to allow the electrospinning of CS solutions that have high conductivity, by reducing the protonation by hydrogen bonding between the amino groups of CS and the ester groups of PEO (Pakravan et al., 2011). The solvent used was acetic acid (Fisher Scientific) 90 % (w/w) in water, and the solutions were stirred overnight in a magnetic stirrer. After obtaining the homogenous solution, citric acid (Sigma-Aldrich), at a concentration equivalent to 30 % (w/w) of the total amount of polymer and dissolved in 1 mL of water, was introduced as a crosslinker. After adding the citric acid solution to the polymeric solution, the mixture was stirred under a magnetic stirrer for 30 min prior to electrospinning. For quercetin-containing FGCS fibers (FGCS-Q), 10 mg of quercetin (Sigma-Aldrich) were added to the citric acid aqueous solution before adding to the final mixture, guaranteeing that the flask was kept out of direct light. The solutions were loaded onto a 5 mL syringe coupled to a 23-gauge needle and then placed on a syringe pump. The distance of the needle tip to the tinfoil-covered collector was 21 cm, the flow rate 0.3 mL/h and the voltage applied between 16 and 18 kV depending on the viscosity of the solution. The process took place at room temperature (20 – 22 °C) and a relative humidity ranging from 45 to 55 %. After electrospinning, to complete the crosslinking process, the electrospun membranes were placed in an oven for 12 h at 100 °C, to completely evaporate the solvent, followed by 3 h at 170 °C.

2.2. Physico-chemical Characterization of electrospun membranes

2.2.1. Scanning Electron Microscopy

The morphology of the fibers was assessed through Scanning Electron Microscopy (SEM) using a Zeiss Auriga Electron Microscope and a TM3030 Plus Hitachi Tabletop Microscope operating in high vacuum at 15 kV. The samples were placed on a metal support using carbon tape and were coated with a 35 nm layer of gold: palladium (60:40). The images were analyzed using the ImageJ software (National Institute of Health, USA) (Schneider et al., 2012). The diameter of at least 70 fibers was measured, and the results were expressed as the average diameter ± experimental standard deviation.

2.2.2. Degradation tests

Hydrolytic degradation of electrospun fibers was assessed over the course of 69 days. 20 mg of FGCS membrane in triplicate were dried in an incubator set to 37 °C and then weighed (Wi). Afterwards, the samples were placed in the degradation medium – PBS pH 7.4 complemented with 0.04 % (w/v) sodium azide (Merck Millipore). Once a week during the first month, the degradation medium was removed, and the samples were thoroughly washed three times with deionized water and left to dry for 48 h in the incubator at 37 °C. After drying, weight measurements were taken (Wk). After the first month, the samples were left in a degradation medium for a full month before taking the final measurement. The results are presented as the average relative remaining mass Wk/Wi ± experimental standard deviation (Vieira et al., 2019).

2.2.3. Fourier Transform Infrared spectroscopy (FTIR)

FTIR was used to evaluate the types of molecular interactions between the different materials. This analysis was performed on a Perking-Elmer Spectrum Two in ATR mode (attenuated total reflectance), and the transmittance spectrum obtained ranged from 4000 cm^{-1} to 400 cm^{-1} in wavenumber.

2.3. Drug delivery and anti-oxidant properties analysis

2.3.1. In vitro drug release assay

To obtain a quercetin calibration curve, the absorbance of different solutions with known concentrations (5, 10, 15, 20, and 25 μg/mL) of quercetin in ethanol was measured using a ScanSpecUV photometer (SCANSCI Ltd) at a wavelength of 376 nm. The encapsulation efficiency (EE) was first calculated to determine the amount of quercetin that is effectively incorporated in the produced fibers. For that, non-crosslinked FGCS-Q fibers were dissolved in 4 mL of water with 100 μL of acetic acid to promote its complete dissolution. Afterwards, the absorbance was measured at 376 nm, and the EE was calculated according to Equation (1), using the mass extrapolated from the calibration curve, where the actual amount of quercetin encapsulated, obtained from measuring the absorbance after dissolving a FGCS-Q fiber, is compared to the theoretical amount of quercetin encapsulated. For the drug delivery assays, electrospun fibers were cut into approximately 5 mg pieces in triplicates and then submerged in 3 mL of release medium. For this purpose, three different release mediums were used: simulated normal skin environment (pH 5.6), phosphate buffer saline (pH 7.4) and simulated wound fluid (pH 8) (Wallace et al., 2019). The fibers were incubated at 37 °C in an orbital shaker, and the absorbance values were measured at a wavelength of 376 nm at several timepoints. After reading the absorbance values, the samples were returned to their respective flasks. For the preparation of the simulated wound fluid, the following components were added to 100 mL of deionized water in order to achieve a pH of 8 ± 0.2: 0.68 g of NaCl, 0.22 g of KCl, 0.35 g of NaH_2PO_4 and 2.5 g of $NaHCO_3$. For the simulated normal skin fluid, 7.721 g of sodium acetate and 352.5 mg of acetic acid were added to 800 mL of deionized water. The pH was adjusted using HCl and NaOH, and then more deionized water was added to reach a final volume of 1 L.

$$Encapsulation\ Efficiency(\%) = \left(\frac{Actual\ amount\ of\ Quercetin\ encapsulated}{Theoretical\ amount\ of\ Quercetin\ encapsulated}\right) \times 100 \quad (1)$$

2.3.2. Anti-oxidant activity

The anti-oxidant activity of pure quercetin and from quercetin-containing fibers was determined using a radical scavenging test with 2,2-diphenyl-1-picrylhydrazyl (DPPH, Sigma-Aldrich). For pure quercetin, 0.5 mL of a quercetin solution was prepared in ethanol by dissolving 125 μg of quercetin, which should correspond to the amount of quercetin present in 5 mg of FGCS-Q fibers. This solution was added to a DPPH solution prepared in ethanol at a concentration of $1x10^{-4}$ M. For FGCS-Q fibers, 5 mg of fiber were placed in a DPPH solution ($1x10^{-4}$ M in ethanol). Both samples were left to react in the dark for 60 min at room temperature, with agitation, and the absorbance was measured at 517 nm. To calculate the antioxidant activity Equation (2) was used, in which *Asample* is the absorbance of a determined sample, and *Acontrol* is the absorbance of the control (ethanol, in this case).

$$Antioxidant\ Activity(\%) = \left(1 - \frac{Asample}{Acontrol}\right) \times 100 \quad (2)$$

2.4. In vitro cellular assays

2.4.1. Cytotoxicity

In vitro tests were performed with the Human Neuroblastoma Cell Line SH-SY5Y (ATCC CRL-2266). To assess potential cytotoxic effects from quercetin as well as from the produced fibers, cytotoxicity assays were used, both direct and indirect approaches, according to the International Standard ISO 10993–5. Firstly, 30,000 cells/cm^2 were seeded using Dulbecco's Modified Eagle's Medium Low Glucose (DMEM, Biowest) supplemented with 10 % fetal bovine serum (FBS, Biowest) and 1 % penicillin–streptomycin (Gibco). After a 24-hour incubation period, both assays were carried out. For the quercetin direct assay, a quercetin solution was prepared in dimethyl sulfoxide (DMSO, Merck Millipore) and diluted in DMEM, to assure a final DMSO concentration of 0.02 %. The starting quercetin concentration used for the assay was 0.5 mM, and consecutive 1:2 dilutions were performed. For the indirect assays, the different fiber samples were previously incubated with fresh medium for 24 h, at a concentration of 15 mg/mL. The extracts were then plated, and consecutive 1:2 dilutions were performed. Fresh DMEM and DMSO at a concentration of 10 % were used as negative and positive controls, respectively. The plates were incubated for 48 h in an MCO-19AIC(UV) CO_2 incubator, in a humidified atmosphere of 5 % CO_2 at 37 °C. To analyze cell viability after exposure to quercetin and the extracts, a resazurin (Alfa Aesar) assay was performed. Resazurin is reduced to resorufin as a result of the metabolic activity of cells. The cells were

exposed to a resazurin solution composed of 50 % complete culture medium and 50 % resazurin solution at a concentration of 0.04 mg/mL in PBS for 3 h, and the absorbance values were read on a Biotek 8000UV reader at the following wavelengths: 600 and 570 nm, corresponding to the maximum absorbance value of resazurin and resorufin, respectively. The corrected absorbance was proportional to cell viability, and the viability was expressed as the percentage of viable cells relative to the negative control.

2.4.2. Adhesion and proliferation

To evaluate SH-SY5Y adhesion and proliferation rates to the produced scaffolds, these were cut into 15 mm disks and sterilized in an oven for 2 h at a temperature of 120 °C. The fiber disks were placed on top of coverslips and secured using O-rings. Cell controls were set by seeding cells directly over the surface of the tissue culture plate wells. Cells were seeded on the top of the membranes at a concentration of 30,000 cells/cm^2 and incubated at 37 °C and 5 % CO_2. Cellular viability was assessed on days 1 (corresponding to cell adhesion), 4, 7, and 10 after seeding, using the resazurin assay similar to the description in the cytotoxicity assay.

2.4.3. Neuronal differentiation

Neuronal differentiation was assessed using different conditions for quercetin . To determine the effect of quercetin on neuronal differentiation, as well as to determine the best concentration, three concentrations were used: 10 μM (Q10), 15 μM (Q15), and 20 μM (Q20). These concentrations were evaluated with DMEM supplemented with 3 % FBS and with DMEM supplemented with 10 % FBS, to assess the effect of quercetin alone, without serum deprivation. As controls, cells exposed to only regular DMEM and cells exposed to 10 μM of retinoic acid (RA, Sigma-Aldrich) in DMEM 3 % were used. For this assay, cells were seeded on top of coverslips at a density of 4000 cells/cm^2. The medium was changed every other day over 7 days.

At the end of the assay, cells were fixed using paraformaldehyde (PFA, Sigma-Aldrich) at a concentration of 4 %, at room temperature for 20 min. These were permeabilized with Triton X-100 (Sigma-Aldrich,0.3 % v/v in PBS) for 15 min and incubated with Bovine Serum Albumin (Biowest, BSA, 2 % in PBS) for 1 h. After this incubation step, the primary antibodies were incubated overnight in their respective samples: MAP2 Monoclonal Antibody (Invitrogen, 1:300) and Beta Tubulin III Monoclonal Antibody (Cell Signaling Technology, 1:200), dissolved in a blocking solution of 1 % BSA and 0.1 % Triton X-100 in PBS. Afterward, the secondary antibodies (Invitrogen) and phalloidin (Proteintech) were dissolved in a blocking solution and incubated in their respective samples for 2 h at room temperature. DAPI (Molecular Probes) was added to every sample at a concentration of 10 nM for 5 min, and then the samples were assembled in coverslips using Mowiol mounting media (Sigma-Aldrich) and imaged with a Nikon Ti-S microscope equipped with an epi-fluorescence module.

2.4.4. Assessment of anti-bacterial activity

To determine the effect of the produced fibers on bacterial growth inhibition, an assay was performed with the reference strains *Escherichia coli* K12 DSM498 (DSMZ, Braunschweig, Germany) and *Staphylococcus aureus* COL MRSA, methicillin-resistant strain (Rockefeller University, USA). The bacterial strains were cultured in Tryptic Soy Broth (TSB, Scharlau) at 37 °C overnight. The samples, FGCS and FGCS-Q fibers at a concentration of 5 mg/mL, were placed in glass tubes with 5 mL of TSB and inoculated with the overnight bacterial culture to a final concentration of approximately 5 x10^5 CFU/mL. A bacterial growth control, without any fiber, was also prepared, and the tubes placed in an incubator at 37 °C for 6 h. After the 6-hour mark, from each tube 10^{-5} and 10^{-6} dilutions were prepared in saline phosphate buffer and then spread in TSB solidified with Agar (Labchem) plates and incubated overnight at 37 °C. The colonies were then counted, and the colony forming units (CFUs) per mL were calculated (Arkoun et al., 2017). Three biological replicates were obtained. The bacterial growth of each sample was normalized to the bacterial control using Equation (3); where Csample is the CFUs/mL of a determined sample, and Ccontrol is the CFUs/mL of the bacterial control.

$$Bacterial\ Growth(\%) = \left(\frac{Csample}{Ccontrol}\right) \times 100 \quad (3)$$

2.5. Statistical analysis

Statistical analysis was performed on the OriginLab software, where One-Way Analysis of Variance (ANOVA) and the Tukey test were used to compare the obtained data. Three different significance levels were used: $p < 0.05$, represented by *; $p < 0.01$, represented by **; and $p < 0.001$, represented by ***.

3. Results and discussion

3.1. SEM

SEM analysis was performed to evaluate fiber morphology and obtain the average diameter values, as well as diameter distribution histograms, which can be consulted in Fig. 1. For FGCS fibers crosslinked with citric acid, the average diameter and respective standard deviation value calculated was 359 ± 71 nm. For FGCS-Q fibers crosslinked with citric acid, the obtained values were FGCS-Q 420 ± 78 nm. Both fibers present a regular shape and a network with a cross pattern that provides porosity without many undesired artifacts. Considering the respective average fiber diameters and the overlapping standard deviations for plane fibers and quercetin-containing fibers, it is possible to infer that adding quercetin does not significantly alter fiber morphology . However, there seems to be a tendency to increase fiber diameter with the addition of quercetin, which is in accordance with studies performed by G. Ajmal *et al.,* where the addition of quercetin to PCL-Gelatin nanofibers resulted in an increased diameter (Ajmal, 2019). Studies have shown that fiber diameter plays an important role in the adhesion and proliferation abilities of the cells, influencing the way they migrate on the provided substrates, as well as regulating neuronal differentiation. G.T. Christopherson *et al.* (2008) demonstrated that a decrease in fiber diameter allowed for increased proliferation and cell spreading, with minimal cell aggregation (Christopherson et al., 2009). Regarding differentiation, different diameters were able to induce different lineages of neuronal cells, where higher fiber diameters of 749 nm promoted an elongated neuronal lineage, and smaller fiber diameters of 283 nm promoted the differentiation into oligodendrocytes (Christopherson et al., 2009). Our fibers present diameter values between those in the previously mentioned article, which allows us to infer that, when inducing neuronal differentiation, a mixture of neuronal cell types might be obtained.

3.2. Degradation tests

Fig. 2 represents the fiber degradation profile of FGCS membranes for 69 days when immersed in PBS. It is possible to observe that the measured weight remained stable during the experiment, with values above 90 %. This suggests that there was an effective crosslinking process from the citric acid, which provided the fibers with the ability to resist hydrolytic degradation over extended periods of time. Any oscillations in the graph can be due to incomplete PBS removal when washing the fibers with deionized before taking the weight measurements, which can increase the measured weight, given the salts that

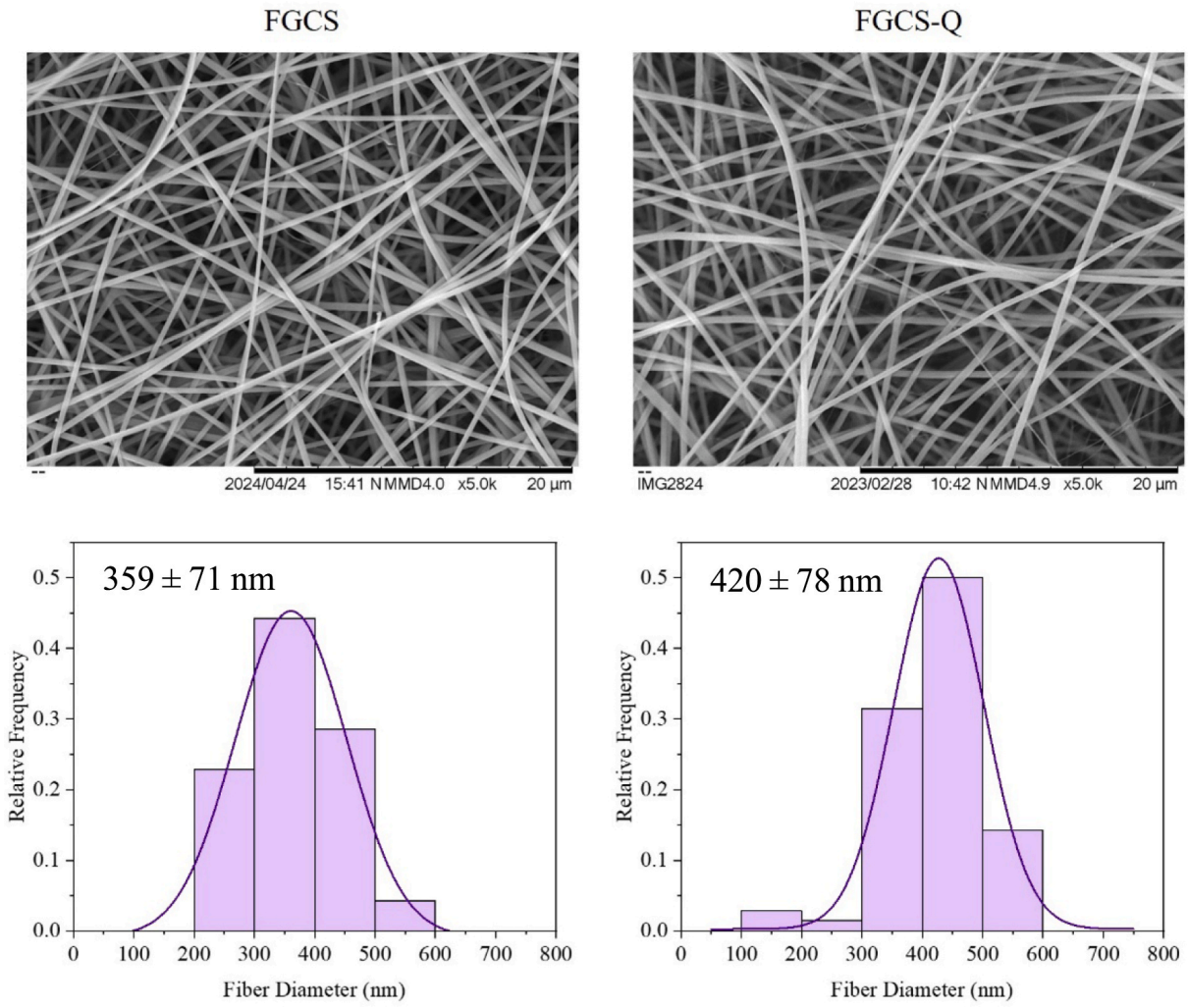

Fig. 1. SEM images of fibers produced by electrospinning and respective diameter distribution graph for FGCS fiber (left) and FGCS-Q fiber (right).

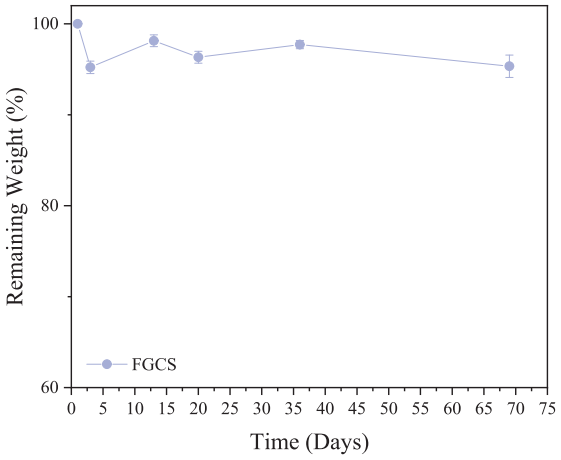

Fig. 2. Degradation profile of FGCS fibers crosslinked with citric acid. The data was acquired from three replicates.

compose PBS. With the barely changed mass over the period of the experiment, it is expected that the degradation of the membranes occurs in bulk and not by erosion. In the bulk degradation, the weight of the samples remain constant over time and then fully disintegrate. However, over the course of the degradation experiment, products with low molecular weight should be released, resulting from FG and CS degradation (Huang et al., 2005).

3.3. FTIR analysis

Given the unique chemical compositions of each material, FTIR spectroscopy can provide a chemical analysis of the samples with the characteristic chemical bonds and vibrational modes, which will allow a better understanding of the materials used and the resultant products. The FTIR spectra obtained can be consulted in Fig. 3. It is possible to observe some gelatin characteristic peaks in FG powder spectrum around the following absorbance bands: 1237 cm^{-1}, related to C – O stretching; 1445 cm^{-1}, from CH_2 stretching; 1534 cm^{-1} and 1630 cm^{-1}, related to amide II (N–H bending vibrations and C-N groups stretching vibrations) and amide I (C = O stretching), respectively; as well as a broad 3284 cm^{-1} band related to O–H and N–H stretching vibrations (Ferreira, 2021; Park and Kim, 2020). For CS powder, it is possible to distinguish some characteristic bands as well, namely: 1580 cm^{-1}, related to primary amines (N–H bending); the broadband at around 3284 cm^{-1}, also related to O–H and N–H stretching; at around 1028–1150 cm^{-1} related to the C-O-C vibrations from chitosan's backbone (Ribeiro et al., 2021; Ferreira, 2021; Ebrahimi et al., 2019). For FGCS and FGCS-Q fibers, the previously mentioned characteristic bands found in FG and CS powders are maintained, even if some slight shifts can be observed due to the interactions of the polymers. In both fibers, it is also possible to observe the appearance of a small band around 1700

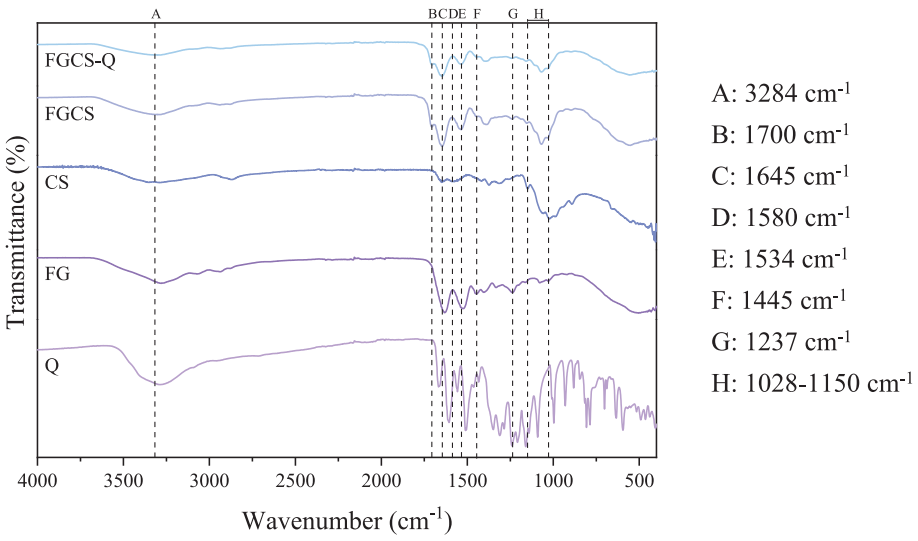

Fig. 3. FTIR spectra of quercetin (Q) powder, fish gelatin (FG) powder, chitosan (CS) powder, FGCS fiber and FGCS-Q fiber.

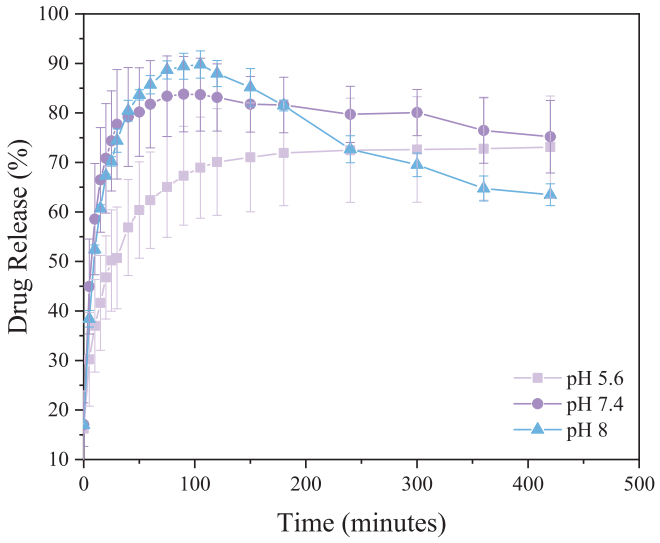

Fig. 4. Quercetin release from FGCS-Q fibers in three different buffers: simulated normal skin environment (pH 5.6), regular PBS (pH 7.4) and simulated wound fluid (pH 8).

cm^{-1}, corresponding to ester bonds, which indicates successful cross-linking with citric acid (Bernadette Agu et al., 2019; Chen, 2025). There does not seem to be a difference in the FGCS-Q spectrum due to the addition of quercetin, which suggests that it is incorporated within the fibrous matrix without establishing chemical interactions with the polymers. Additionally, the equipment might not be able to detect alterations due to the low quantities.

3.4. Drug delivery

The encapsulation efficiency of quercetin in the FGCS membranes was calculated using Equation (1), indicating a 46.9 ± 0.99 % encapsulation efficiency, and for the drug release studies, the maximum amount encapsulated used to convert the release data in percentage was 58.6 μg. The drug release profile (%) of the FGCS-Q fibers can be observed in Fig. 4, which represents the amount of quercetin released from the electrospun fibers as a function of time over 420 min and then at 1440 min (the 24 h time point, not shown in Fig. 4). The experiment was performed in different buffers: one that simulates a normal skin environment (pH 5.6), one that simulates wound fluid (pH 8), and regular PBS (pH 7.4) (Wallace et al., 2019). The highest values obtained for each release medium were 73.10 %, 83.81 %, and 89.90 % for pH 5.6, pH 7.4 and pH 8, respectively. Regarding the pH 5.6 release medium, there was a slower release over time, reaching nearly the maximum amount after the 100-minute mark, whereas for the pH 7.4 release medium, the release profile indicates a rapid release during the first 50 min. For the pH 8 release medium, the maximum amount was reached at around 100 min, followed by a decrease over time, indicating quercetin's degradation in the release medium. Although there was not a significant difference in the quercetin release in the different pH for larger times, which can be due to the degradation of quercetin, for short times up to 100 min, there is a significant difference in the release of quercetin in pH 5.6 when compared to pH 8. Studies have shown that quercetin exhibits higher instability in mild alkaline and alkaline solutions, supporting the observed degradation at pH 8 (Osojnik Črnivec, 2024). It is also possible to observe a slight degradation at pH 7.4. However, it is not as pronounced as what happens at pH 8. Furthermore, a higher release in an acidic medium should be expected, given that there is a higher FG dissolution in acidic conditions, as well as a higher CS dissolution due to its positive charges that promote the opening of the fiber network in acidic conditions (Herdiana et al., 2022). This increased dissolution of the polymers in acidic conditions can lead to a more enhanced quercetin release from the fiber network to the release medium. However, that was not verified in this experiment since release media with pH 7.4 and pH 8 exhibited a higher drug release when compared to pH 5.6, which would be beneficial since it could guarantee a more pronounced release at the wound site instead of normal, healthy skin. This can be due to the bulk degradation of the electrospun fibers, reported in section 3.2, which allows the easy penetration of the PBS in the fibers followed by a release of low molecular weight byproducts. As the degradation proceeds, the deeper regions of the fibers are exposed, which can accelerate the release before reach the plateau. Thus, the observed pseudo-parabolic release of quercetin involves the combination of surface-bound drug diffusion and the release by degradation, presenting a behavior that does not fit the standard diffusion models alone (Paolella et al., 2024). This release profile is particularly beneficial for chronic wounds, as the initial burst provides immediate protection during the early inflammatory phase following tissue injury, while the subsequent sustained release ensures prolonged delivery of the extract (Ferreira, 2021). Furthermore, given quercetin's instability in an aqueous environment, providing a carrier can increase its availability and stability (Osojnik Črnivec, 2024). Form our system, the amount of

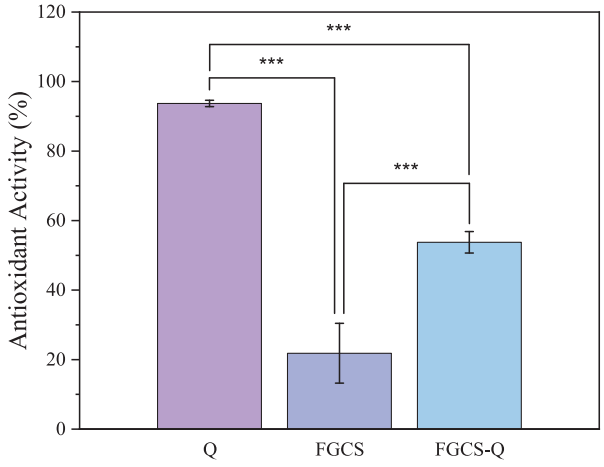

Fig. 5. Antioxidant activity from pure quercetin (Q), FGCS fibers and FGCS-Q fibers. The results were statistically compared to each other using ANOVA for three different significance levels: $p < 0.05$, represented by *; $p < 0.01$, represented by **; and $p < 0.001$, represented by ***.

quercetin that can be released from the fibers corresponds to 19 μg/mL (100 % release). From previous studies (Ajmal, 2019; Zhou, 2021; Nayak, 2025), the effective local concentration of quercetin should be in the range of 10 to 50 μ g/mL for application in a small wound area (1 cm^2). Although the values are near the low limit, the *in vitro* studies showed promising results of using this system in wound healing applications.

3.5. Antioxidant activity

The antioxidant activity assay allowed to determine the antioxidant properties of pure quercetin and compare them with the antioxidant properties of plain fibers and fibers containing quercetin. The results in Fig. 5 indicate an antioxidant activity of 93.71 ± 0.92 % for pure quercetin, 21.83 ± 8.60 % for FGCS fibers and 53.77 ± 3.09 % for FGCS-Q fibers. Overall, these findings can demonstrate the excellent antioxidant properties of pure quercetin, as well as quercetin-containing fibers. Even though there is a lower antioxidant activity for FGCS-Q fibers, this can be related to the encapsulation process of quercetin into the fibers, as well as its potential degradation during the production process, resulting in a decreased amount of available quercetin than what would be expected. As discussed in the drug delivery section, the encapsulation efficiency of quercetin within the fibers is around 46.9 %, which can support the decrease in antioxidant activity when compared with pure quercetin since the amount of quercetin used was equivalent to the theoretical amount that should have been encapsulated in the fibers. FGCS fibers still present some antioxidant activity but are much lower than FGCS-Q fibers. This slight antioxidant activity can be related to CS, which has been shown to have antioxidant properties (Park et al., 2004). Although the study was conducted with synthetic polymers, Paolella and co-workers found similar values of quercetin antioxidant activity in PCL and polyvinylpyrrolidone electrospun membranes encapsulated with quercetin (Paolella et al., 2024). Another study using electrospun membranes from synthetic polymers, PLA and poly(ethylene glycol), with quercetin, showed a superior antioxidant activity (80 %) (Stoyanova, 2025). With natural polymers, Roy et al. used CS and gelatin polymers that were processed in the form of fims, using genipin as crosslinker, and were encapsulated with quercetin. The antioxidant activity for this system was lower (30 %) than the one reported in our study (54 %), when the DPPH method was used (Roy and Rhim, 2022). The use of electrospun membranes with high surface area allows more expousure of DPPH to quercetin, increasing the antioxidant activity. Overall, the results indicate that adding quercetin to the fibers enhanced their antioxidant activity by almost threefold. Quercetin's antioxidant activity has been studied, and its mechanism of action is derived from the existence of polyphenolic components (Roy and Rhim, 2022; Yadav et al., 2020). It is crucial for this application that the produced fibers can aid in removing reactive oxygen species at the wound site since these free radicals can cause damage in the axons of neurons present in the area (André-Lévigne et al., 2024). These damages can highly impair the production of important neuropeptides essential in efficient skin wound healing (Ashrafi et al., 2016).

3.6. Cytotoxicity

Resazurin assay weas performed to assess the potential cytotoxic effects of quercetin and the produced fibers on SH-SY5Y cells from the neuroblastoma cell line. According to ISO 10993–5, cell viability above 80 % is considered non-toxic, 60–80 % is lightly toxic, 40–60 % is moderately toxic, and below 40 % is severely toxic (López-García et al.,

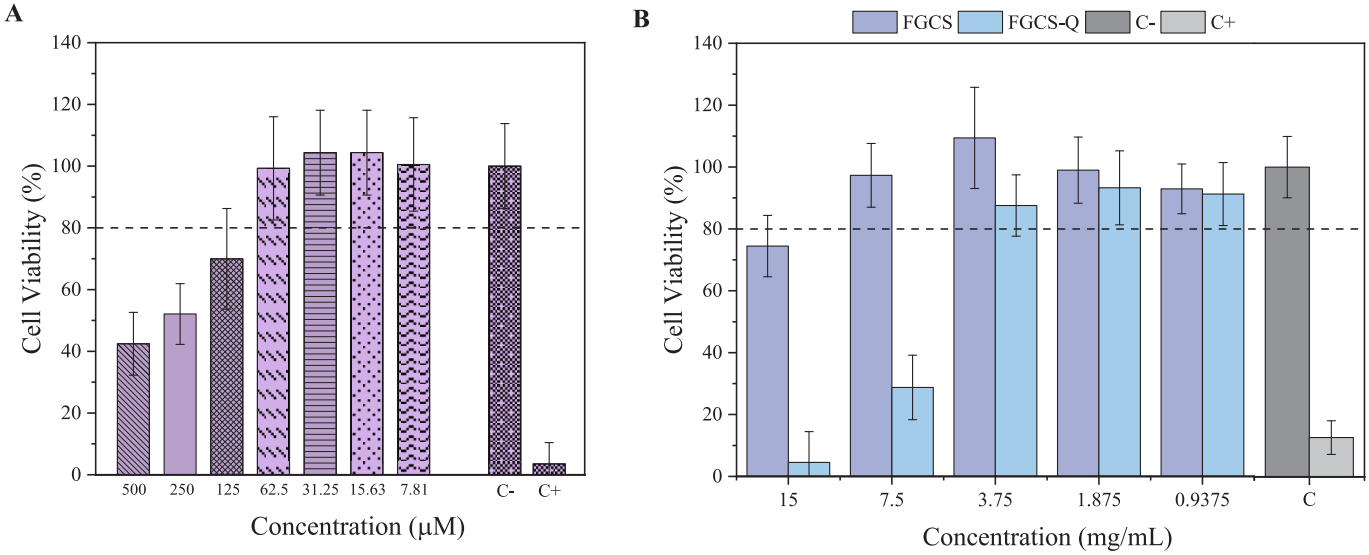

Fig. 6. SH-SY5Y cell viability after a 48-hour incubation period with: (A) quercetin in sequential 1:2 dilutions; (B) different fiber extracts in sequential 1:2 dilutions. The line at 80 % represents the threshold at which there are no cytotoxic effects. The data obtained for both experiments is derived from three biological replicates and the results were normalized to the negative control.

2014). The graphic in Fig. 6A represents the cytotoxic effects of 48 hours quercetin exposure on SH-SY5Y cells, starting from a concentration of 500 μM to 7.81 μM, in sequential 1:2 dilutions. It is possible to observe that at a concentration of 500 μM, cell viability is close to 40 %, presenting severe toxic effects, whereas at a concentration of 250 μM show moderate toxicity, with cell viability around 50 %. At a concentration of 125 μM, the viability shows light toxicity, with viability close to 70 %. Lower concentrations ranging from 62.5 μM to 7.81 μM show viability percentages above 80 %, demonstrating minimal to no cytotoxic effects. The low viability values for the positive control and high values for the negative control confirm that the test was properly sensitive to cell viability.

The cytotoxicity of the produced membranes towards neuronal cells was studied by exposing cells to fiber extracts for 48 h in the following concentrations: 15 mg/mL, 7.5 mg/mL, 3.75 mg/mL, 1.875 mg/mL, and 0.9375 mg/mL. The results can be consulted in Fig. 6B. The obtained graph shows that at a concentration of 15 mg/mL, FGCS fibers present viability percentages close to 80 %, indicating minimal cytotoxicity. In contrast, FGCS-Q fibers present severe toxicity with very low viability percentages, suggesting cytotoxic action from quercetin at this concentration. For the rest of the concentrations, FGCS fibers present viability values above 80 %, being absent from cytotoxic effects. On the other hand, FGCS-Q fibers still present cytotoxic effects at a concentration of 7.5 mg/mL, only becoming non-cytotoxic from 3.75 mg/mL and below.

3.7. Adhesion and proliferation

To infer the membranes' ability to promote cell adhesion and proliferation, an assay was performed over 10 days for three different biological replicates. After seeding the cells for 24 h, the first evaluation was performed through a resazurin assay, which established first-day viability, corresponding to the adhesion ratio, and further measurements were taken for 10 days to determine the proliferation ratio. The results obtained can be observed in Fig. 7. The adhesion ratio for FGCS and FGCS-Q was 30 ± 14 % and 16 ± 18 %, respectively, and can be consulted in Table 1, alongside the proliferation values. For both membranes and the cell control (CC), there was an increase in cell proliferation throughout the experiment. The proliferation ratio from day 1 to day 10 demonstrates the lower proliferation ratio for FGCS-Q compared to FGCS and CC. Regarding quercetin's effect, there is a decrease in cell proliferation for FGCS-Q fibers compared with FGCS fibers. However, it is still possible to observe an increase in proliferation. Relating to the cytotoxicity of fiber extracts presented before, it is possible to conclude that the adhesion and proliferation results obtained should not be related to the cytotoxicity imposed by the fibers since the fiber concentration in the medium obtained in this proliferation assay was lower than 3.75 mg/mL, which corresponds to the concentration at which none of the fibers are considered cytotoxic. Nevertheless, these results show that cells were able to adhere to the scaffolds, proliferate, and maintain a stable population throughout the experiment.

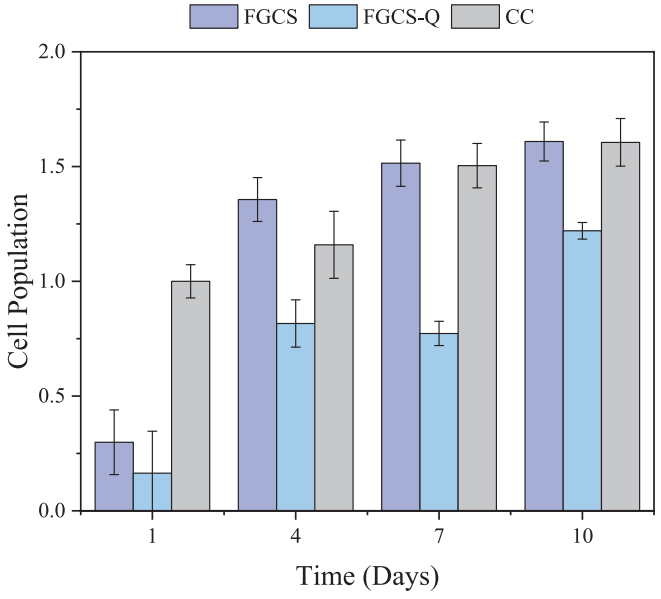

Fig. 7. Cell adhesion and proliferation for SH-SY5Y cells seeded in the different fiber mats. Viability measurements were taken on days 1, 4, 7 and 10 after seeding. The obtained results refer to three biological replicates and were normalized to first day control population.

Table 1
Adhesion and proliferation ratios for SH-SY5Y cells. The adhesion ratio of SH-SY5Y is shown for the 3 different samples, and the proliferation ratio is obtained by dividing the cell population from day 10 by the cell population from day 1.

Membranes	Adhesion Ratio	Proliferation
FGCS	30 ± 14	5.5 ± 0.6
FGCS-Q	16 ± 18	8.2 ± 0.9
CC	100 ± 7	2.2 ± 0.2

3.8. Neuronal differentiation

Immunofluorescence staining was performed to assess the differentiation ability of SH-SY5Y neuronal cells under different conditions. Different concentrations of quercetin were used to observe the influence it has on inducing neuronal differentiation: 10 μM (Q10), 15 μM (Q15), and 20 μM (Q20). Furthermore, these concentrations were applied to cells under DMEM supplemented with 10 % FBS (D10%) to assess quercetin's effect alone, as well as cells under DMEM supplemented with 3 % FBS (D3%), which has been shown to aid in neuronal differentiation. As controls, cells subjected only to D10% and D3% were used, as well as cells subjected to serum deprivation (D3%) with 10 μM of RA since these conditions have been proven to induce neuronal differentiation in SH-SY5Y cells (Shipley et al., 2016). MAP2 and β-III Tubulin were used as neuronal markers to perform the immunofluorescence staining, and DAPI was used for nuclear staining. The differentiation was assessed by analyzing the morphological differences present in the different samples. As can be observed in Figs. 8 and 9, cells exposed to quercetin and retinoic acid present a more elongated, neuron-like morphology, whereas cells present in controls CD3% and CD10% maintain a retracted phenotype with short projections, suggesting that there was limited differentiation (Shipley et al., 2016). In both cases, for D3% and D10%, an increase in quercetin concentration resulted in a lower cellular density due to the low proliferation rate of neurons undergoing differentiation. Furthermore, it is also possible to observe some neurite-like extensions. Overall, the obtained images suggest that quercetin alone can induce neuronal differentiation. However, the experiment's time length is insufficient to infer much more about its efficacy. Regarding RA control, there is a more evident differentiation and more neurite-like extensions in the same period, indicating that quercetin may take longer to induce differentiation when compared to RA. It is also possible to note a difference in intensity regarding the neuronal markers, where β-III Tubulin shows a lower intensity than MAP2, which could be related to the fact that β-III Tubulin is recognized as a marker for more mature neurons, whereas MAP2 has been shown to increase its expression in a short period of time (Mohamad Nasir et al., 2024; Cheung, 2009). Nonetheless, these results are promising and further increase quercetin's potential to be used as an API destined for skin regeneration and reinnervation in chronic skin wounds.

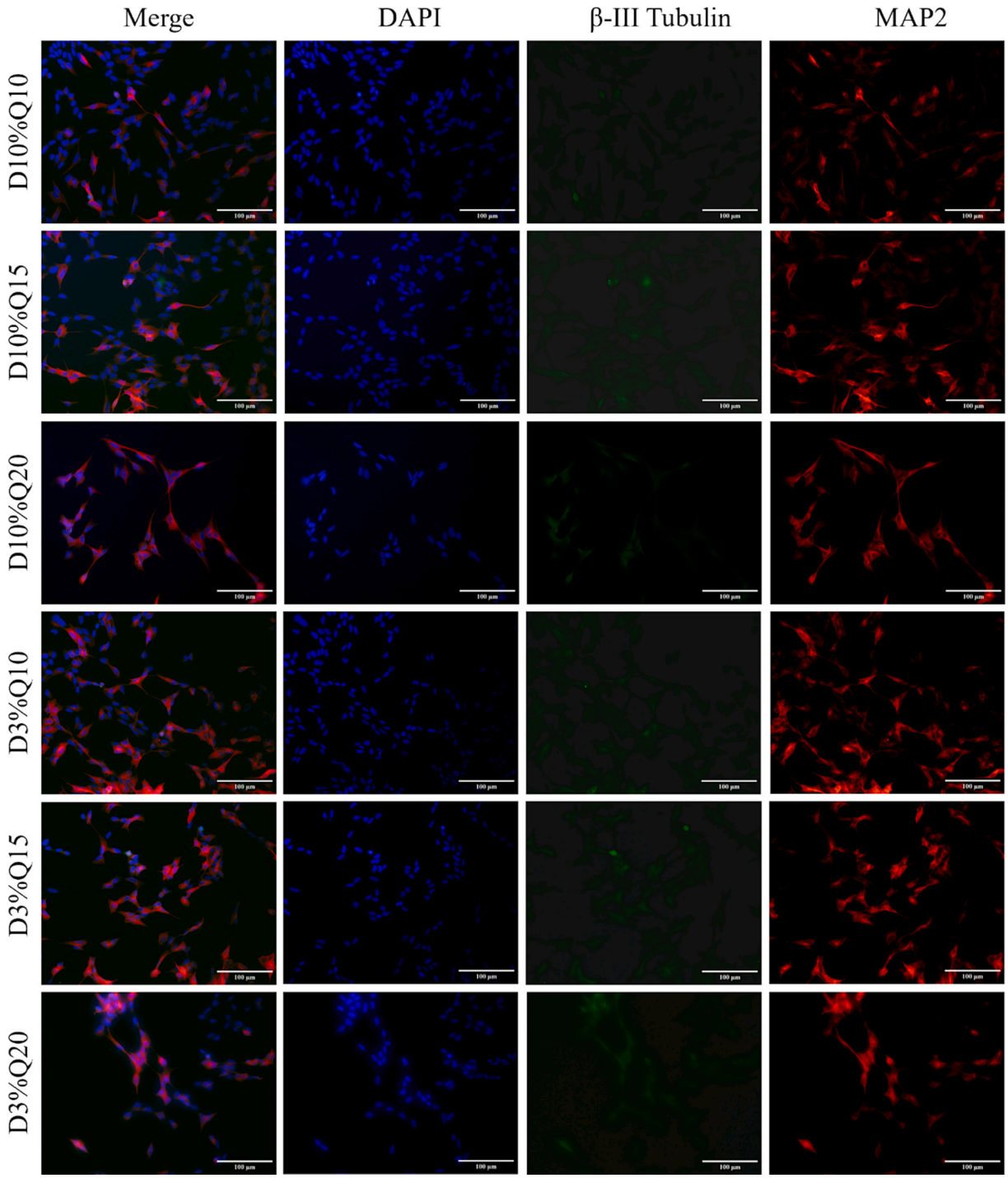

Fig. 8. Immunofluorescence staining of SH-SY5Y cells at day 7 of being exposed to different differentiation conditions. Cells were stained with DAPI, β-III Tubulin and MAP2. Images were obtained at 40 X magnification using an inverted microscope equipped with an epi-fluorescence module. Scale bar 100 μm.

3.9. Antibacterial activity

Fig. 10 shows the bacterial growth from *E. coli* (left) and MRSA (right) when exposed to FGCS and FGCS-Q fibers. These results were normalized to the bacterial control without the presence of any additional fibers. As such, we can better understand the effect that fibers have on bacterial growth. Referring to the MRSA growth graph (Fig. 10, right), it is possible to attribute a bacterial effect to both membranes. Even though there is a decrease in bacterial growth when comparing the control with FGCS fibers, there is a greater emphasis on the bacterial growth decrease for FGCS-Q fibers compared to the control and FGCS fibers. The introduction of plain FGCS provided a bacterial growth decrease of around 40 %, which can be attributed to CS's bacterial activity. CS's antibacterial activity has been highly demonstrated, and its action mode has been attributed to its positive charge, provided by the positively charged amino groups (Yilmaz Atay, 2020; Kong et al., 2010; Pereda et al., 2011). These positive charges interact with the negatively charged membranes present in bacteria, leading to their destruction and leakage of several intracellular components (Yilmaz Atay, 2020; Kong et al., 2010; Pereda et al., 2011). However, there was a decrease of around 90 % for FGCS-Q fibers, which adds up to 50 % more than FGCS fibers, which confirms that the addition of quercetin provided an even

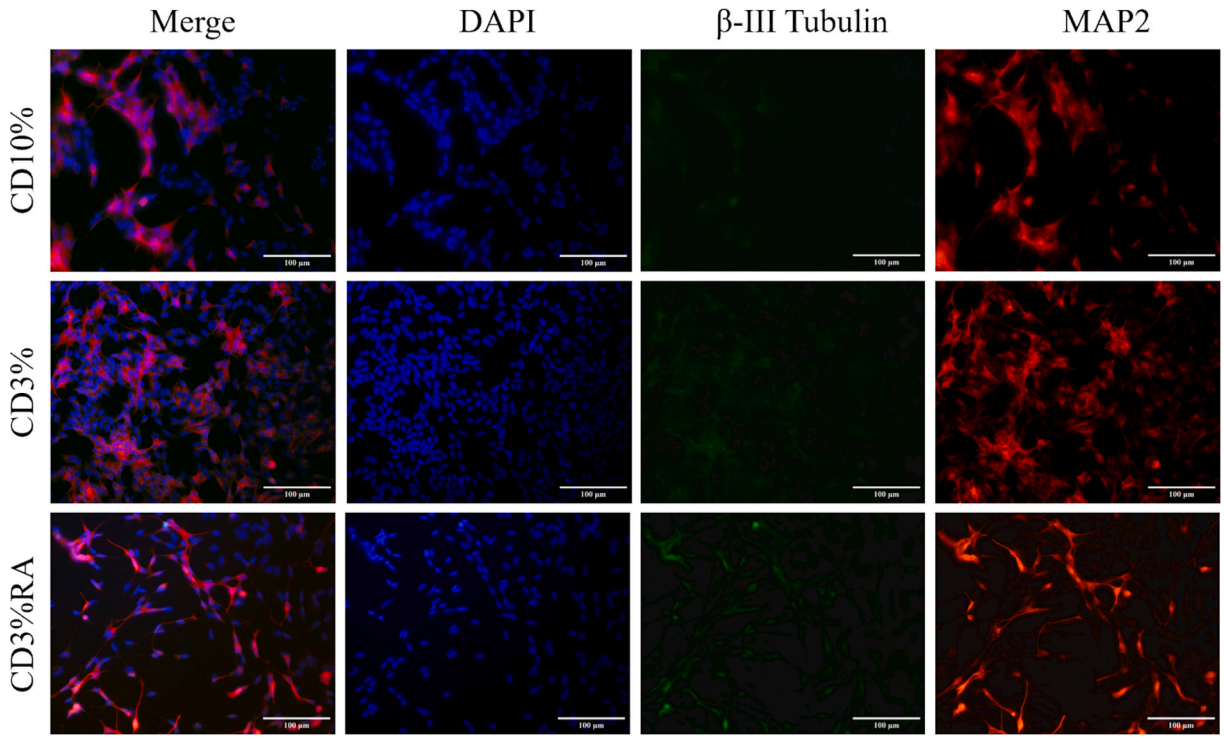

Fig. 9. Immunofluorescence staining of SH-SY5Y cells at day 7 of being exposed to different differentiation conditions. Cells were stained with DAPI, β-III Tubulin and MAP2. Images were obtained at 40 X magnification using an inverted microscope equipped with an epi-fluorescence module. Scale bar 100 μ m.

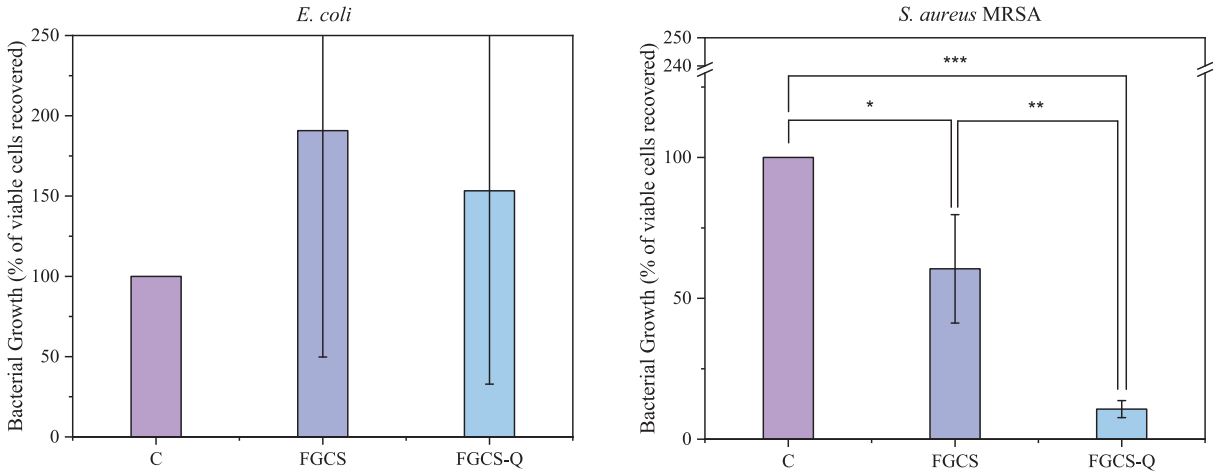

Fig. 10. Effect of FGCS and FGCS-Q on the growth of *E. coli* and *S. aureus* MRSA. The results were statistically compared to each other using ANOVA for three different significance levels: $p < 0.05$, represented by *; $p < 0.01$, represented by **; and $p < 0.001$, represented by ***. The data represented accounts for three biological replicates for *E. coli* and four biological replicates for *S. aureus* MRSA. In this last case, two outliers were removed, one for FGCS and another for FGCS-Q samples.

more accentuated antibacterial effect. Quercetin's antibacterial effects have also been demonstrated, and they have been attributed to an increase in membrane permeability to ions, which leads to the loss of membrane potential (Mirzoeva et al., 1997). As can be observed in the graph relative to *E. coli* growth (Fig. 10, left), there are no statistically significant changes to the bacterial growth when comparing the fibers with the control, as well as between both fibers. Therefore, we can not attribute any antibacterial effects to the fibers towards *E. coli*. Several studies have shown not only CS's antibacterial effect towards this strain but also quercetin's positive antibacterial actions, which lead us to believe that higher concentrations of either polymer or API are required, or the concentration of 5 mg/mL used for the experiment was not enough to show significant results for *E. coli* (Wiggers, 2022). Furthermore, studies performed with both these strains showed a decreased, or even inexistent antibacterial effect towards *E. coli* when compared to MRSA (Wiggers, 2022; Kanatt et al., 2012), which can explain the fact that it is possible to see an impact towards MRSA and not *E. coli* at the used concentrations. It was suggested that the lipopolysaccharides present in the cell wall of Gram-negative bacteria could prevent the active components from reaching the cytoplasmic membrane, thus decreasing their antibacterial effects (Kanatt et al., 2012).

4. Conclusions

In this study, electrospun FG and CS fibers crosslinked with citric acid, incorporating quercetin, were successfully produced. These scaffolds demonstrated a uniform morphology and porous structure, capable of sustaining hydrolytic degradation. Drug release assays showed a higher quercetin release at pH 7.4 and pH 8, which corresponds to typical wound site conditions. However, quercetin degradation at a more alkaline pH suggests an additional encapsulation step is needed to preserve its stability and proper effects. Antioxidant activity analysis confirmed quercetin's outstanding free radical scavenging activity, presenting values of 93.71 ± 0.92 % for pure quercetin, and 53.77 ± 3.09 % for quercetin-containing fibers. Neuronal differentiation assays demonstrated the API's potential in promoting neuronal differentiation, an essential condition for proper wound recovery. Nonetheless, further studies are required to understand its effects. Finally, antibacterial tests indicated that incorporating quercetin effectively reduced MRSA growth but had no significant effect on *E. coli*. Overall, these findings reveal quercetin's potential as a suitable API for chronic skin wound regeneration and reinnervation due to its antioxidant, antibacterial, and neurogenic properties. Further studies should focus on optimizing quercetin's stabilization through its encapsulation and further elucidate its role in neuronal differentiation in its pure form and incorporated in the produced fibers, unraveling long-term biological effects in proper models.

CRediT authorship contribution statement

Catarina Correia: Writing – original draft, Methodology, Investigation, Data curation. **Ana Sofia Pádua:** Methodology, Investigation. **Catarina Matela:** Methodology, Investigation. **Inês C. Gonçalves:** Methodology, Investigation. **Paula Soares:** Writing – review & editing, Resources, Data curation. **Célia Henriques:** Writing – review & editing, Supervision, Resources. **Isabel Sá-Nogueira:** Writing – review & editing, Supervision, Resources, Funding acquisition, Data curation. **Jorge Carvalho Silva:** Writing – review & editing, Supervision, Resources, Data curation. **Tânia Vieira:** Writing – review & editing, Supervision, Resources, Project administration, Funding acquisition, Data curation.

Declaration of competing interest

The authors declare that they have no known competing financial interests or personal relationships that could have appeared to influence the work reported in this paper.

Acknowledgements

This research was funded by the FCT – Fundação para a Ciência e a Tecnologia, I.P., in the scope of the projects 2022.07258.PTDC (123SkinHeal) and the projects LA/P/0037/2020, UIDP/50025/2020 and UIDB/50025/2020 of the Associate Laboratory Institute of Nanostructures, Nanomodelling and Nanofabrication-i3N. It was also funded by FCT – Fundação para a Ciência e a Tecnologia, I.P., in the scope of the project UIDP/04378/2020 and UIDB/04378/2020 of the Research Unit on Applied Molecular Biosciences - and the project LA/P/0140/2020 of the Associate Laboratory Institute for Health and Bioeconomy - i4HB.

Data availability

Data will be made available on request.

References

Abrigo, M., McArthur, S.L., Kingshott, P., 2014. Electrospun nanofibers as dressings for chronic wound care: advances, challenges, and future prospects. Macromol. Biosci. 14, 772–792.

Agarwal, S., Wendorff, J. H. & Greiner, A. Use of electrospinning technique for biomedical applications. *Polymer* vol. 49 5603–5621 Preprint at Doi: 10.1016/j.polymer.2008.09.014 (2008).

Ajmal, G., et al., 2019. Biomimetic PCL-gelatin based nanofibers loaded with ciprofloxacin hydrochloride and quercetin: a potential antibacterial and anti-oxidant dressing material for accelerated healing of a full thickness wound. Int. J. Pharm. 567, 118480.

André-Lévigne, D. *et al.* Role of Oxygen and Its Radicals in Peripheral Nerve Regeneration: From Hypoxia to Physoxia to Hyperoxia. *International Journal of Molecular Sciences* vol. 25 Preprint at Doi: 10.3390/ijms25042030 (2024).

Arkoun, M., Daigle, F., Heuzey, M.C., Ajji, A., 2017. Antibacterial electrospun chitosan-based nanofibers: a bacterial membrane perforator. Food Sci. Nutr. 5, 865–874.

Armstrong, D.G., Wrobel, J., Robbins, J.M., 2007. Guest editorial: are diabetes-related wounds and amputations worse than cancer? Int. Wound J. 4, 286–287.

Ashrafi, M., Baguneid, M. & Bayat, A. The role of neuromediators and innervation in cutaneous wound healing. *Acta Dermato-Venereologica* vol. 96 587–597 Preprint at Doi: 10.2340/00015555-2321 (2016).

Azimi, B. *et al.* Bio-based electrospun fibers for wound healing. *Journal of Functional Biomaterials* vol. 11 Preprint at Doi: 10.3390/JFB11030067 (2020).

Bernadette Agu, A. S., Japheth Benablo, P. L., D Mesias, V. S. & Penaloza Jr, D. P. *Synthesis and characterization of a chitosan-based citric acid-crosslinked encapsulant system. J. Chil. Chem. Soc* vol. 64 (2019).

Bhardwaj, N. & Kundu, S. C. Electrospinning: A fascinating fiber fabrication technique. *Biotechnology Advances* vol. 28 325–347 Preprint at Doi: 10.1016/j.biotechadv.2010.01.004 (2010).

Chen, M.M., et al., 2017. Quercetin promotes motor and sensory function recovery following sciatic nerve-crush injury in C57BL/6J mice. J. Nutr. Biochem. 46, 57–67.

Chen, J., et al., 2025. Mechanistic Study on Citric Acid-based Esterification: a Versatile Reaction for Preparation of Hydrophilic Polymers. ACS Sustain. Chem. Eng. 13, 559–570.

Cheung, Y.T., et al., 2009. Effects of all-trans-retinoic acid on human SH-SY5Y neuroblastoma as in vitro model in neurotoxicity research. Neurotoxicology 30, 127–135.

Christopherson, G.T., Song, H., Mao, H.Q., 2009. The influence of fiber diameter of electrospun substrates on neural stem cell differentiation and proliferation. Biomaterials 30, 556–564.

Cui, C. *et al.* Electrospun chitosan nanofibers for wound healing application. *Engineered Regeneration* vol. 2 82–90 Preprint at Doi: 10.1016/j.engreg.2021.08.001 (2021).

Da Silva Uebel, L., et al., 2016. Quercetin and curcumin in nanofibers of polycaprolactone and poly(hydroxybutyrate-co-hydroxyvalerate): Assessment of in vitro antioxidant activity. J. Appl. Polym. Sci. 133.

Darie-Niță, R. N., Râpă, M. & Frąckowiak, S. Special Features of Polyester-Based Materials for Medical Applications. *Polymers* vol. 14 Preprint at Doi: 10.3390/polym14050951 (2022).

Ebrahimi, S., Fathi, M., Kadivar, M., 2019. Production and characterization of chitosan-gelatin nanofibers by nozzle-less electrospinning and their application to enhance edible film's properties. Food Packag. Shelf Life 22.

Eskitoros-Togay, M., Bulbul, Y.E., Dilsiz, N., 2018. Quercetin-loaded and unloaded electrospun membranes: Synthesis, characterization and in vitro release study. J Drug Deliv Sci Technol 47, 22–30.

Ferreira, C.A.M., et al., 2021. Multifunctional gelatin/chitosan electrospun wound dressing dopped with undaria pinnatifida phlorotannin-enriched extract for skin regeneration. Pharmaceutics 13.

Ficai, D., Albu, M. G., Sonmez, M., Ficai, A. & Andronescu, E. Advances in the field of soft tissue engineering: From pure regenerative to integrative solutions. in *Nanobiomaterials in Soft Tissue Engineering: Applications of Nanobiomaterials* 355–386 (Elsevier Inc., 2016). doi:10.1016/B978-0-323-42865-1.00013-1.

Fideles, S. O. M. *et al.* Influence of the Neuroprotective Properties of Quercetin on Regeneration and Functional Recovery of the Nervous System. *Antioxidants* vol. 12 Preprint at Doi: 10.3390/antiox12010149 (2023).

Girard, D., et al., 2017. Biotechnological Management of Skin Burn Injuries: challenges and Perspectives in Wound Healing and Sensory Recovery. Tissue Eng. B Rev. 23, 59–82.

Herdiana, Y., Wathoni, N., Shamsuddin, S. & Muchtaridi, M. Drug release study of the chitosan-based nanoparticles. *Heliyon* vol. 8 Preprint at Doi: 10.1016/j.heliyon.2021.e08674 (2022).

Huang, Y., Onyeri, S., Siewe, M., Moshfeghian, A., Madihally, S.V., 2005. In vitro characterization of chitosan–gelatin scaffolds for tissue engineering. Biomaterials 26, 7616–7627.

Hulupi, M. & Haryadi, H. *Synthesis and Characterization of Electrospinning PVA Nanofiber-Crosslinked by Glutaraldehyde. Materials Today: Proceedings* vol. 13 www.sciencedirect.comwww.materialstoday.com/proceedings (2019).

Kanatt, S.R., Rao, M.S., Chawla, S.P., Sharma, A., 2012. Active chitosan-polyvinyl alcohol films with natural extracts. Food Hydrocoll. 29, 290–297.

Karuppannan, S.K., et al., 2022. Quercetin functionalized hybrid electrospun nanofibers for wound dressing application. Mater Sci Eng B Solid State Mater Adv Technol 285.

Kong, M., Chen, X. G., Xing, K. & Park, H. J. Antimicrobial properties of chitosan and mode of action: A state of the art review. *International Journal of Food Microbiology* vol. 144 51–63 Preprint at Doi: 10.1016/j.ijfoodmicro.2010.09.012 (2010).

Kost, B., et al., 2020. PLA/β-CD-based fibres loaded with quercetin as potential antibacterial dressing materials. Colloids Surf. B Biointerfaces 190.

Liguori, A., et al., 2019. Electrospinning of fish gelatin solution containing citric acid: an environmentally friendly approach to prepare crosslinked gelatin fibers. Materials 12.

López-García, J., Lehocký, M., Humpolíček, P., Sáha, P., 2014. HaCaT keratinocytes response on antimicrobial atelocollagen substrates: extent of cytotoxicity, cell viability and proliferation. J Funct Biomater 5, 43–57.
Mathew, S.A., Arumainathan, S., 2022. Crosslinked chitosan-gelatin biocompatible nanocomposite as a neuro drug carrier. ACS Omega 7, 18732–18744.
Mirzoeva, O.K., Grishanin, R.N., Calder, P.C., 1997. Antimicrobial action of propolis and some of its components: the effects on growth, membrane potential and motility of bacteria. Microbiol. Res. 152, 239–246.
Mohamad Nasir, N.F., Mohd Hazli, M.S.H., Shamsuddin, S., Zainuddin, A., 2024. Alteration of mature neuronal marker of β-III tubulin expression in differentiated SH-SY5Y cells by refinement of foetal bovine serum concentration. Beni Suef Univ J Basic Appl Sci 13.
Mohammadi, M.R., Rabbani, S., Bahrami, S.H., Joghataei, M.T., Moayer, F., 2016. Antibacterial performance and in vivo diabetic wound healing of curcumin loaded gum tragacanth/poly(ε-caprolactone) electrospun nanofibers. Mater. Sci. Eng. C 69, 1183–1191.
Nayak, M., et al., 2025. Quercetin nanocrystal-loaded alginate hydrogel patch for wound healing applications. J. Mater. Chem. B 13, 1690–1703.
Oryan, A., Alidadi, S., Bigham-Sadegh, A., Moshiri, A., 2016. Comparative study on the role of gelatin, chitosan and their combination as tissue engineered scaffolds on healing and regeneration of critical sized bone defects: an in vivo study. J. Mater. Sci. - Mater. Med. 27.
Osojnik Črnivec, I.G., et al., 2024. Aspects of quercetin stability and its liposomal enhancement in yellow onion skin extracts. Food Chem. 459.
Pakravan, M., Heuzey, M.-C., Ajji, A., 2011. A fundamental study of chitosan/PEO electrospinning. Polymer (guildf) 52, 4813–4824.
Paolella, G., Montefusco, A., Caputo, I., Gorrasi, G., Viscusi, G., 2024. Quercetin encapsulated polycaprolactone-polyvinylpyrrolidone electrospun membranes as a delivery system for wound healing applications. Eur. J. Pharm. Biopharm. 200.
Park, P.J., Je, J.Y., Kim, S.K., 2004. Free radical scavenging activities of differently deacetylated chitosans using an ESR spectrometer. Carbohydr. Polym. 55, 17–22.
Park, S.H., Kim, J.C., 2020. Complexation-responsive monoolein cubic phase containing extract of Bambusae Caulis in Taeniam. Int. J. Polym. Mater. Polym. Biomater. 69, 44–52.
Pereda, M., Ponce, A.G., Marcovich, N.E., Ruseckaite, R.A., Martucci, J.F., 2011. Chitosan-gelatin composites and bi-layer films with potential antimicrobial activity. Food Hydrocoll. 25, 1372–1381.
Ribeiro, A.S., Costa, S.M., Ferreira, D.P., Abidi, H., Fangueiro, R., 2021. Development of chitosan-gelatin nanofibers with cellulose nanocrystals for skin protection applications. *Key Engineering Materials*. (Trans Tech Publications Ltd.
Roy, S., Rhim, J.W., 2022. Genipin-Crosslinked Gelatin/Chitosan-based Functional Films Incorporated with Rosemary Essential Oil and Quercetin. Materials 15.
Schiffman, J.D., Schauer, C.L., 2007. Cross-linking chitosan nanofibers. Biomacromolecules 8, 594–601.
Schneider, C. A., Rasband, W. S. & Eliceiri, K. W. NIH Image to ImageJ: 25 years of image analysis. *Nature Methods* vol. 9 671–675 Preprint at Doi: 10.1038/nmeth.2089 (2012).
Shipley, M.M., Mangold, C.A., Szpara, M.L., 2016. Differentiation of the SH-SY5Y human neuroblastoma cell line. J. Vis. Exp. 2016.
Song, W., et al., 2024. Quercetin Alleviates Diabetic Peripheral Neuropathy by Regulating Axon Guidance Factors and Inhibiting the Rho/ROCK Pathway in vivo and in vitro. Diabetes, Metabolic Syndrome and Obesity 17, 4339–4354.
Stoyanova, N., et al., 2022. Quercetin- and rutin-containing electrospun cellulose acetate and polyethylene glycol fibers with antioxidant and anticancer properties. Polymers (basel) 14.
Stoyanova, N., et al., 2025. The effect of Quercetin Loading in Polylactic Acid-based Electrospun Fibers on their Antioxidant. Antibacterial and Antitumor Properties. Molecules 30.
Trinh, X. T. *et al.* A Comprehensive Review of Natural Compounds for Wound Healing: Targeting Bioactivity Perspective. *International Journal of Molecular Sciences* vol. 23 Preprint at Doi: 10.3390/ijms23179573 (2022).
Vieira, T., Carvalho Silva, J., Botelho do Rego, A. M., Borges, J. P. & Henriques, C. Electrospun biodegradable chitosan based-poly(urethane urea) scaffolds for soft tissue engineering. *Materials Science and Engineering C* **103**, (2019).
Wallace, L. A., Gwynne, L. & Jenkins, T. Challenges and opportunities of pH in chronic wounds. *Therapeutic Delivery* vol. 10 719–735 Preprint at Doi: 10.4155/tde-2019-0066 (2019).
Wiggers, H.J., et al., 2022. Quercetin-Crosslinked Chitosan Films for Controlled Release of Antimicrobial Drugs. Front. Bioeng. Biotechnol. 10.
Yadav, S., Mehrotra, G.K., Bhartiya, P., Singh, A., Dutta, P.K., 2020. Preparation, physicochemical and biological evaluation of quercetin based chitosan-gelatin film for food packaging. Carbohydr. Polym. 227.
Yao, Z., Niu, J., Cheng, B., 2020. Prevalence of Chronic Skin Wounds and their Risk Factors in an Inpatient Hospital setting in Northern China. Adv. Skin Wound Care 33, 1–10.
Yilmaz Atay, H. Antibacterial activity of chitosan-based systems. in *Functional Chitosan: Drug Delivery and Biomedical Applications* 457–489 (Springer Singapore, 2020). doi: 10.1007/978-981-15-0263-7_15.
Zhong, S. P., Zhang, Y. Z. & Lim, C. T. Tissue scaffolds for skin wound healing and dermal reconstruction. *Wiley Interdisciplinary Reviews: Nanomedicine and Nanobiotechnology* vol. 2 510–525 Preprint at Doi: 10.1002/wnan.100 (2010).
Zhou, L., et al., 2021. Electrospun chitosan oligosaccharide/polycaprolactone nanofibers loaded with wound-healing compounds of Rutin and Quercetin as antibacterial dressings. Int. J. Biol. Macromol. 183, 1145–1154.